# Reactions of [*t*-$Bu_2SnO$]$_3$ with [*t*-$BuX_2Si$]$_2$ (X = F, Cl). Syntheses and Structures of Novel Stannasiloxanes and of [(*t*-$Bu_2FSn)_2O$]$_2$, the First Fluorine-Containing Tetraorganodistannoxane[||,⊥]

**Jens Beckmann,[†] Monique Biesemans,[‡] Karl Hassler,[§] Klaus Jurkschat,*,[†] Jose C. Martins,[‡] Markus Schürmann,[†] and Rudolph Willem*,[‡]**

Lehrstuhl für Anorganische Chemie II, Universität Dortmund, D-44221 Dortmund, Germany, High-Resolution NMR Centre (HNMR), Free University of Brussels (VUB), Pleinlaan 2, B-1050 Brussel, Belgium, and Institute for Inorganic Chemistry, Technical University of Graz, Stremayrgasse 16, A-8010 Graz, Austria

*Received December 2, 1997*

Di-*tert*-butyltin oxide, (*t*-$Bu_2SnO)_3$ (**1**), reacts with 1,2-di-*tert*-butyltetrachlorodisilane, (*t*-$BuCl_2Si)_2$ (**2**), to provide the stannasiloxane *t*-$Bu_2Sn[OSi(OSnCl$-*t*-$Bu_2)$-*t*-$Bu]_2$ (**4**, racemate). The reaction of **1** with 1,2-di-*tert*-butyltetrafluorodisilane, (*t*-$BuF_2Si)_2$ (**3**), provides the stannasiloxane [*t*-Bu(F)SiOSn-*t*-$Bu_2]_2O$ (**5**, meso/racemate mixture) and the tetraorganodistannoxane [*t*-$Bu_2$(F)SnOSn(F)-*t*-$Bu_2]_2$ (**6**). Under loss of $^1/_3$ mole equiv of **1**, the stannasiloxane **5** is transformed into *t*-$Bu_2Sn[OSi(F)$-*t*-BuSi(F)-*t*-$BuO]_2Sn$-*t*-$Bu_2$ (**7**). Its ten-membered ring structure was elucidated by X-ray analysis. In solution, **7** forms the five-membered ring *t*-$Bu_2Sn[OSi(F)$-*t*-$Bu]_2$ (**7a**). The dimeric nature of **6** was confirmed by its crystal structure determination. In solution, **6** exhibits a unique valence tautomerism as evidenced by $^{19}F$ and $^{119}Sn$ NMR spectroscopy.

## Introduction

Although the first stannasiloxane was reported as early as 1952,[1] systematic studies appeared only recently on formation, structures, and reactivity of such systems containing Si−O−Sn units.[2] Compounds of this type are of potential interest as models for mixed-metal oxide surfaces and might allow the control of the formation of tin silicate molecular sieves and related materials.[3] Cyclic stannasiloxanes hold potential as molecular precursors for well-defined polystannasiloxanes.[2n] A general synthetic approach to stannasiloxanes is the reaction of organosilanols with organochlorostannanes in the presence of a base,[2c,h,k,n] the reaction of organosilanols with organotin oxides,[2h] or lithium halide elimination from organosilanolates and organohalostannanes.[2a,b,f,g,i] The particularly high Brønsted acidity of silica surfaces allows cleavage of Sn−C and Sn−H bonds, respectively, and formation of Si−O−Sn linkages.[3a,c,e] In preliminary studies, Davies and Harrison reported reactions of organochlorosilanes with polymeric diorganotin oxides ($R_2SnO)_n$ (R = Me, Bu) that provided stannasiloxanes, but the products were not completely characterized.[1j,l]

Recently, we showed that, in reactions with organosilanes such as *t*-$BuSiF_3$ and *t*-$Bu_2SiX_2$ (X = F, Cl), (*t*-$Bu_2SnO)_3$, hereafter referred to as **1**, is a convenient synthon for the high-yield preparation of well-defined stannasiloxanes such as *t*-$Bu_2Sn[OSi(F)$-*t*-$Bu_2]_2$, [(*t*-$Bu_2SiO$)(*t*-$Bu_2SnO)_2$], and [(*t*-BuRSiO)(*t*-

[†] Universität Dortmund.
[‡] Free University of Brussels.
[§] Technical University of Graz.
[||] Dedicated to Professor Marcel Gielen on the occasion of his 60th birthday.
[⊥] This paper contains part of the intended Ph.D. thesis of Jens Beckmann, Dortmund University.

(1) (a) Tatlock, W. S.; Rochow, E. G. *J. Org. Chem.* **1952**, *17*, 1555. (b) Okawara, R. *Angew. Chem.* **1961**, *73*, 383. (c) Okawara, R.; White, D. G.; Fujitani, K.; Sato, H. *J. Am. Chem. Soc.* **1961**, *83*, 1342. (d) Kochkin, D. A.; Chirzadze, Y. N. *J. Gen. Chem. (USSR)* **1962**, *32*, 3932. (e) Thies, C.; Kinsinger, J. B. *Inorg. Chem.* **1964**, *3*, 551. (f) Schmidbaur, H.; Hussek, H. *J. Organomet. Chem.* **1964**, *1*, 244. (g) Considine, W. J.; Baum, G. A.; Jones, R. C. *J. Organomet. Chem.* **1965**, *3*, 308. (h) Schmidbaur, H. *Angew. Chem.* **1965**, *77*, 206. (i) Hayashi, K.; Iyoda, J.; Shiihara, I. *J. Organomet. Chem.* **1967**, *10*, 81. (j) Davies, A. G.; Harrison, P. G. *J. Organomet. Chem.* **1967**, *10*, P31. (k) Davies, A. G.; Harrison, P. G.; Silk, T. A. G. *Chem. Ind. (London)* **1968**, 949. (l) Davies, A. G.; Harrison, P. G. *J. Chem. Soc. C* **1971**, 1769.

(2) (a) Morosin, B.; Harrah, L. A. *Acta Crystallogr.* **1981**, *B37*, 579. (b) Graalmann, O.; Meyer, M.; Klingebiel, U. *Z. Anorg. Allg. Chem.* **1986**, *534*, 109. (c) Feher, F. J.; Newman, D. A.; Walzer, J. F. *J. Am. Chem. Soc.* **1989**, *111*, 1741. (d) Brown, P.; Mahon, M. F.; Molloy, K. C. *J. Chem. Soc., Dalton Trans.* **1990**, 2643. (e) McGeary, M. J.; Cayton, R. H.; Folting, K.; Huffman, J. C.; Caulton, K. G. *Polyhedron* **1992**, *11*, 1369. (f) Sipyagina, M. A.; Vasetchenkova, T. V.; Polyakova, M. V.; Ivashchenko, D. A.; Stepanova, E. E.; Buzyreva, N. M.; Chernyshev, E. A. *Russ. J. Gen. Chem. (Engl. Transl.)* **1993**, *63*, 1114. (g) Schütte, S.; Klingebiel, U.; Schmidt-Bäse, D. *Z. Naturforsch.* **1993**, *48B*, 263. (h) Brisdon, B. J.; Mahon, M. F.; Molloy K. C.; Schofield, P. J. *J. Organomet. Chem.* **1994**, *465*, 145. (i) Abrahams, I.; Montevalli, M.; Shah S. A. A.; Sullivan, A. C. *J. Organomet. Chem.* **1995**, *492*, 99. (j) Xin, F.; Pope, M. T.; Long, G. J.; Russo, U. *Inorg. Chem.* **1996**, *35*, 1207. (k) Voigt, A.; Murugavel, R.; Roesky, H. W. *Organometallics* **1996**, *15*, 5097. (l) Jurkschat, K.; Rosche, F.; Schürmann, M. *Phosphorus, Sulfur Silicon* **1996**, *115*, 161. (m) Sita, L. R.; Xi, R.; Yap, G. P. A.; Liable-Sands, L. M.; Rheingold, A. L. *J. Am. Chem. Soc.* **1997**, *119*, 756. (n) Beckmann, J.; Jurkschat, K.; Schollmeyer, D.; Schürmann, M. *J. Organomet. Chem.* **1997**, *543*, 229.

(3) (a) Mansour, A. E.; Candy, J. P.; Bournonville, J. P.; Ferretti, O. A.; Basset, J. M. *Angew. Chem.* **1989**, *101*, 360. (b) Voronkova, V. M.; Voronkov, M. G. *J. Appl. Chem. USSR (Engl. Transl.)* **1992**, *65*, 735. (c) Nédez, C.; Theolier, A.; Lefebvre, F.; Choplin, A.; Basset, J. M.; Joly, J. F. *J. Am. Chem. Soc.* **1993**, *115*, 722. (d) Clark, E. N.; Harrison, P. G. *J. Organomet. Chem.* **1993**, *463*, 85. (e) Nédez, C.; Choplin. A.; Lefebvre, F.; Basset, J. M. *Inorg. Chem.* **1994**, *33*, 1099. (f) Buffon, R.; Schuchardt, U.; Abras, A. *J. Chem. Soc., Faraday Trans.* **1995**, *91*, 3511. (g) Das, T. K.; Chaudhari, K.; Chandwadkar, A. J.; Sivasanker, S. *J. Chem. Soc., Chem. Commun.* **1995**, 2495. (h) Hirao, Y.; Yokoyama, C.; Misono, M. *J. Chem. Soc., Chem. Commun.* **1996**, 597.

S0020-1669(97)01504-8 CCC: $15.00 © 1998 American Chemical Society
Published on Web 09/01/1998

$Bu_2SnO)]_2$ (R = *t*-Bu, F).[4] As a continuation of these studies, we present here our first results on the reaction of **1** with tetrahalodisilanes ($t$-$BuX_2Si)_2$ (**2**, X = Cl; **3**, X = F). Also reported is the unexpected formation of $[(t\text{-}Bu_2FSn)_2O]_2$, the first fluorine-containing tetraorganodistannoxane.

## Experimental Section

All manipulations were carried out under an atmosphere of dry nitrogen. Reagent grade solvents were dried by standard procedures and distilled prior to use. $(t\text{-}BuSiCl_2)_2$,[5] $(t\text{-}BuSiF_2)_2$,[5] and $(t\text{-}Bu_2SnO)_3$[6] were prepared according to literature methods.

NMR spectra were recorded in $CDCl_3$ at room temperature on a Bruker AMX 500 spectrometer at 500.13 ($^1$H), 125.8 ($^{13}$C), 99.4 ($^{29}$Si), and 186.5 ($^{119}$Sn) MHz using $Me_4Si$ and $Me_4Sn$ as external references. The $^{19}$F NMR spectra were recorded on a Bruker AC 250 instrument tuned at 235.35 MHz, using $CFCl_3$ as the external reference. The 2D $^1$H−$^{119}$Sn and $^{19}$F−$^{117}$Sn HMQC spectra were recorded as explained previously.[7a,c]

The mass spectra were obtained on a Finnigan MAT 8230 spectrometer. Ions showed the expected isotope patterns. No molecular ions were observed, which is typical for *tert*-butyl-containing organoelement compounds.[7d] The osmometric molecular weight measurements were performed in chloroform using a Knaur osmometer. The elemental analyses were performed on an instrument from Carlo Erba Strumentazione (model 1106). The density of single crystals of **7** was determined using a Micromeritics Accu Pyc 1330.

**Synthesis of 3,4-Bis(di-*tert*-butylchlorostannoxy)-1,1,3,4-tetra-*tert*-butyl-2,5-dioxa-3,4-disila-1-stannacyclopentane (4).** A mixture of $(t\text{-}BuSiCl_2)_2$ (624 mg, 2 mmol) and $(t\text{-}Bu_2SnO)_3$ (1.99 g, 2.67 mmol) was heated at reflux in $CHCl_3$ (5 mL) for 24 h. The solvent was evaporated in vacuo, and the $t$-$Bu_2SnCl_2$ was removed by sublimation under reduced pressure. After cooling to −78 °C, the remaining oil solidified to give 1.6 g (80%) of **4** as an amorphous solid, mp 85 °C. Anal. Calcd for $C_{32}H_{72}Cl_2O_4Si_2Sn_3$: C, 38.3; H, 7.2. Found: C, 38.5; H, 8.3. $^1$H NMR ($\delta$): 1.43 ppm (18H, $^3J(^1H-^{119}Sn)$ = 109.2 Hz, Sn−*t*-Bu), 1.41 ppm (18H, $^3J(^1H-^{119}Sn)$ = 106.9 Hz, Sn−*t*-Bu), 1.38 ppm (18H, $^3J(^1H-^{119}Sn)$ = 97.0 Hz, Sn−*t*-Bu), 1.10 ppm (18H, $^3J(^1H-^{29}Si)$ = 6.4 Hz, Si−*t*-Bu). $^{13}C\{^1H\}$ NMR ($\delta$): 42.4 ppm ($^1J(^{13}C-^{119}Sn)$ = 456 Hz, Sn−*C*Me$_3$), 41.9 ppm ($^1J(^{13}C-^{119}Sn)$ = 450 Hz, Sn−*C*Me$_3$), 39.4 ppm $^1J(^{13}C-^{119}Sn)$ = 466 Hz, Sn−*C*Me$_3$), 30.2 ppm (Sn−C*Me*$_3$), 29.9 ppm (Sn−C*Me*$_3$), 29.8 ppm (Sn−C*Me*$_3$), 27.1 ppm (Si−C*Me*$_3$), 21.6 ppm ($^1J(^{13}C-^{29}Si)$ = 64.4 Hz, $^3J(^{13}C-^{119/117}Sn)$ = 13.4 Hz, Si−*C*Me$_3$). $^{29}Si\{^1H\}$ NMR ($\delta$): −14.3 ppm ($^2J(^{29}Si-^{119}Sn)$ = 112.1 Hz, $^1J(^{29}Si-^{13}C)$ = 65.2 Hz, $^2J(^{29}Si-^{119}Sn)$ = 12.3 Hz). $^{119}Sn\{^1H\}$ NMR ($\delta$): −49.9 ppm (2Sn, $^1J(^{119}Sn-^{13}C)$ = 453 Hz, $^2J(^{119}Sn-^{29}Si)$ = 112 Hz), −88.8 ppm (1Sn, $^1J(^{119}Sn-^{13}C)$ = 467 Hz).

Mass spectrum, *m*/*z* (assignment, relative intensity): 734 ($C_{24}H_{53}ClO_4Si_2Sn_2$, 15%), 642 ($C_{20}H_{44}O_4Si_2Sn_2$, 10%), 620 ($C_{16}H_{35}ClO_4Si_2Sn_2$, 10%), 586 ($C_{16}H_{36}O_4Si_2Sn_2$, 13%), 508 ($C_8H_{19}ClO_4Si_2Sn_2$, 8%), 472 ($C_8H_{18}O_4Si_2Sn_2$, 23%), 354 ($C_8H_{18}O_4Si_2Sn$, 10%), 57 ($C_4H_9$, 100%).

**Synthesis of 5,6-Difluoro-1,1,3,3,5,6-hexa-*tert*-butyl-2,4,7-trioxa-5,6-disila-1,3-distannacycloheptane (5) and 1,3-Difluoro-tetra-*tert*-butyldistannoxane (6).** A mixture of $(t\text{-}BuSiF_2)_2$ (493 mg, 2 mmol) and $(t\text{-}Bu_2SnO)_3$ (1.99 g, 2.67 mmol) was heated at reflux in $CHCl_3$ (5 mL) for 24 h. After the mixture was cooled to room temperature, the precipite of **6** (960 mg, 92%; mp 250 °C dec) was removed by filtration and the solvent was evaporated to give **5** (1.31 g, 91%; mp 125 °C dec) as a colorless solid. Anal. Calcd for **5**, $C_{24}H_{54}O_3F_2Si_2Sn_2$: C, 39.9; H, 7.5. Found: C, 39.4; H, 8.2. Osmometric molecular weight determination (10 mg/mL of $CHCl_3$): 717 (calcd 722). $^1$H NMR ($\delta$): 1.37 ppm (18H, $^3J(^1H-^{119}Sn)$ = 96.2 Hz, Sn−*t*-Bu), 1.36 ppm (18H, $^3J(^1H-^{119}Sn)$ = 100.9 Hz, Sn−*t*-Bu), 0.96 ppm (18H, $^3J(^1H-^{29}Si)$ = 6.6 Hz, Si−*t*-Bu). $^{13}C\{^1H\}$ NMR ($\delta$): 38.6 ppm ($^1J(^{13}C-^{119}Sn)$ = 505 Hz, Sn−*C*Me$_3$), 38.5 ppm ($^1J(^{13}C-^{119}Sn$ = 523 Hz, Sn−*C*Me$_3$), 29.9, 29.4 ppm (Sn−C*Me*$_3$), 24.8 ppm (Si−C*Me*$_3$), 20.4 ppm ($^2J(^{13}C-^{19}F)$ = 5.3 Hz, Si−*C*Me$_3$). $^{19}F\{^1H\}$ NMR ($\delta$): −134.2 ppm ($^1J(^{19}F-^{29}Si)$ = 377, 315 Hz). $^{29}Si\{^1H\}$ NMR ($\delta$): −12.0 ppm ($^1J(^{29}Si-^{19}F)$ = 346 Hz, $^2J(^{29}Si-^{119/117}Sn)$ = 74.1 Hz, $^2J(^{29}Si-^{19}F)$ = 58.3 Hz). $^{119}Sn\{^1H\}$ NMR ($\delta$): −121.2 ppm ($^2J(^{119}Sn-^{117}Sn)$ = 612 Hz, $^1J(^{119}Sn-^{13}C)$ = 513, 497 Hz, $^2J(^{119}Sn-^{29}Si)$ = 76.2 Hz).

Mass spectrum, *m*/*z* (assignment, relative intensity): 664 ($C_{20}H_{44}O_3F_2Si_2Sn_2$, 14%), 608 ($C_{16}H_{36}O_3F_2Si_2Sn_2$, 20%), 550 ($C_{12}H_{26}O_3F_2Si_2Sn_2$, 6%), 494 ($C_8H_{18}O_3F_2Si_2Sn_2$, 11%), 476 ($C_8H_{19}O_3FSi_2Sn_2$, 10%), 438 ($C_4H_{10}O_3F_2Si_2Sn_2$, 5%), 376 ($C_8H_{18}O_3F_2Si_2Sn_2$, 8%), 361 ($C_8H_{19}O_2F_2Si_2Sn$, 8%), 57 ($C_4H_9$, 100%).

Anal. Calcd for **6**, $C_{32}H_{72}O_2F_4Sn_4$: C, 37.0; H, 7.0. Found: C, 36.0; H, 7.7. $^{119}Sn\{^1H\}$ NMR ($\delta$): −226.3 ppm ($^1J(^{119}Sn-^{19}F)$ = 807 Hz, $^2J(^{119}Sn-^{117}Sn)$ = 110 Hz), 290.4 ppm ($^1J(^{119}Sn-^{19}F)$ = 2450 Hz, $^2J(^{119}Sn-^{117}Sn)$ = 110 Hz).

**Synthesis of 1,1,3,4,6,6,8,9-Octa-*tert*-butyl-3,4,8,9-tetrafluoro-2,5,7,10-tetraoxa-3,4,8,9-tetrasila-1,6-distannacyclodecane (7).** A solution of **5** (1.08 g, 1.5 mmol) in hexane (50 mL) was passed through a Celite column (3 cm × 10 cm). The solvent was removed in vacuo to give a solid residue, which was recrystallized from hexane to provide colorless crystals of **7** (210 mg, 30%; mp 157 °C). Anal. Calcd for $C_{32}H_{72}F_4O_2Si_4Sn_2$: C, 40.6; H, 7.7. Found: C, 40.5; H, 8.3. Osmometric molecular weight determination (10 mg/mL of $CHCl_3$): 473 (calcd 473). $^1$H NMR ($\delta$): 1.39 ppm (18H, $^3J(^1H-^{119}Sn)$ = 104.2 Hz, Sn−*t*-Bu), 0.99 ppm (Si−*t*-Bu). $^{13}C\{^1H\}$ NMR ($\delta$): 40.9 ppm (Sn−*C*Me$_3$), 28.5 ppm (Sn−C*Me*$_3$), 24.1 ppm (Si−C*Me*$_3$), 18.7 ppm ($^2J(^{13}C-^{19}F)$ = 5.7 Hz, Si−*C*Me$_3$). $^{19}F\{^1H\}$ NMR ($\delta$): −139.9 ppm. $^{29}Si\{^1H\}$ NMR ($\delta$): −7.3 ppm ($^1J(^{29}Si-^{19}F)$ = 353 Hz, $^2J(^{29}Si-^{19}F)$ = 52.3 Hz, $^2J(^{29}Si-^{119/117}Sn)$ = 16.3 Hz). $^{119}Sn\{^1H\}$ NMR ($\delta$): −95.0 ppm ($^1J(^{119}Sn-^{13}C)$ = 430 Hz).

Mass spectrum, *m*/*z* (assignment, relative intensity): 851 ($C_{28}H_{63}F_2O_4Si_4Sn_2$, 42%), 812 ($C_{28}H_{62}O_4Si_4Sn_2$, 5%), 767 ($C_{24}H_{55}F_2O_4Si_3Sn_2$, 12%), 717 ($C_{24}H_{52}FO_4Si_2Sn_2$, 6%), 660 ($C_{20}H_{43}FO_4Si_2Sn_2$, 8%), 542 ($C_{12}H_{28}O_3Si_3Sn_2$, 15%), 524 ($C_{20}H_{44}O_4Si_2Sn$, 12%), 474 ($C_{16}H_{36}F_2O_2Si_2Sn$, 33%), 418 ($C_{12}H_{28}F_2O_2Si_2Sn$, 5%), 361 ($C_8H_{19}F_2O_2Si_2Sn$, 28%), 57 ($C_4H_9$, 100%).

**Crystallography.** Intensity data for the colorless crystals (blocks of 0.40 × 0.30 × 0.30 mm (**6**) and 0.30 × 0.15 × 0.15 mm (**7**)) were collected on a Nonius KappaCCD diffractometer with graphite-monochromated MoK$\alpha$ radiation. The data collection covered almost the whole sphere of reciprocal space with 360 frames via $\omega$-rotation ($\Delta/\omega$ = 1°) at two times 5 s for **6** and 10 s for **7** per frame. The crystal-to-detector distance was 2.6 cm. Crystal decay was monitored by repeating the initial frames at the end of data collection. In analyzing the duplicate reflections, there was no indication for any decay. The data were not corrected for absorption effects. The structure was solved by direct methods SHELXS86[8] and successive difference Fourier syntheses. Refinement applied full-matrix least-squares methods SHELXL93[9].


(4) (a) Beckmann, J.; Jurkschat, K.; Schollmeyer, D.; Schürmann, M. *XIth International Symposium on Organosilicon Chemistry*, Montpellier, France, Sept 1−6, 1996; Abstract OA13. (b) Jurkschat, K. *XIIth FECHEM Conference on Organometallic Chemistry*, Prague, Aug 31−Sept 5, 1997; Abstract PL11. (c) Beckmann, J.; Biesemans, M.; Hassler, K.; Jurkschat, K.; Martins, J.; Schürmann, M.; Willem, R. *XIIth FECHEM Conference on Organometallic Chemistry*, Prague, Aug 31−Sept 5, 1997; Abstract PA68. (d) Beckmann, J.; Jurkschat, K.; Schollmeyer, D.; Schürmann, M. *4th Anglo/German Inorganic Chemistry Meeting*, Marburg, Germany, Sept 14−17, 1997; Abstract 47. (e) Jurkschat, K.; Beckmann, J.; Schollmeyer, D.; Schürmann, M. *26th GDCh Annual General Meeting and 100th Anniversary of GÖCh*,Vienna, Sept 7−11, 1997; Abstract AC-NM6. (f) Beckmann, J.; Jurkschat, K.; Schollmeyer, D. In *Organosilicon Chemistry III. From Molecules to Materials*; Auner, N., Weis, J., Eds.; Whiley-VCH: New York, 1998; p 403. (g) Beckmann, J.; Jurkschat, K.; Mahieu, B.; Schürmann, M. *Main Group Met. Chem.* **1998**, *21*, 113.

(5) Reiter, B.; Hassler, K. *J. Organomet. Chem.* **1994**, *467*, 21.

(6) Puff, H.; Schuh, W.; Sievers, R.; Wald, W.; Zimmer, R. *J. Organomet. Chem.* **1984**, *260*, 271.

(7) (a) Pieper, N.; Klaus-Mrestani, C.; Schürmann, M.; Jurkschat, K.; Biesemans, M.; Verbruggen, I.; Martins, J. C.; Willem, R. *Organometallics* **1997**, *16*, 1043. (b) Willem, R.; Bouhdid, A.; Kayser, F.; Delmotte, A.; Gielen, M.; Martins, J. C.; Biesemans, M.; Mahieu, B.; Tiekink, E. R. T. *Organometallics* **1996**, *15*, 1920. (c) Laatikainen, R.; Niemitz, M.; Malaisse, W. J.; Biesemans, M.; Willem, R. *Magn. Reson. Med.* **1996**, *36*, 359. (d) Weidenbruch, M.; Pesel, H.; Van Hieu, D. *Z. Naturforsch.* **1980**, *35B*, 31.

**Table 1.** Crystal Data and Structure Refinement for **6** and **7**

| | | |
|---|---|---|
| empirical formula | $C_{32}H_{72}F_4O_2Sn_4 \cdot 2CHCl_3$ (**6**) | $C_{32}H_{72}F_4O_4Si_4Sn_2$ (**7**) |
| fw | 1278.39 | 946.65 |
| $T$, °C | 18(1) | 18(1) |
| $\lambda$, Å | 0.710 69 | 0.710 69 |
| space group | $P\bar{1}$ (No. 2) | $P\bar{1}$(No. 2) |
| $a$, Å | 11.284(1) | 9.706(1) |
| $b$, Å | 11.926(1) | 11.732(1) |
| $c$, Å | 12.282(1) | 11.818(1) |
| $\alpha$, deg | 79.801(1) | 114.010(1) |
| $\beta$, deg | 61.736(1) | 92.040(1) |
| $\gamma$, deg | 63.368(1) | 108.230(1) |
| $V$, Å$^3$ | 1300.0(1) | 1146.8(2) |
| $Z$ | 1 | 1 |
| $\rho_{obsd}$, g cm$^{-3}$ | 1.633 | 1.371 |
| $\rho_{calcd}$, g cm$^{-3}$ | not measd | 1.407(5) |
| $\mu$, cm$^{-1}$ | 22.47 | 12.39 |
| R1 ($I > 2\sigma(I)$) ($F$)$^a$ | 7.39 | 3.47 |
| wR2 (all data) ($F^2$)$^b$ | 23.02 | 7.78 |

$^a$ R1 $= \sum||F_o| - |F_c||/\sum|F_o|$. $^b$ wR2 $= [\sum[w(F_o^2 - F_c^2)^2]/\sum[w(F_o^2)^2]]^{0.5}$.

**Table 2.** Selected Bond Lengths (Å), Angles (deg) and Torsion Angles (deg) for **7**$^a$

| | | | |
|---|---|---|---|
| Sn(1)−O(2) | 1.969(2) | Sn(1)−O(1) | 1.975(2) |
| Sn(1)−C(1) | 2.166(4) | Sn(1)−C(5) | 2.167(4) |
| Si(1)−O(1) | 1.605(3) | Si(1)−F(1) | 1.610(2) |
| Si(1)−C(11) | 1.883(4) | Si(1)−Si(2a) | 2.3772(14) |
| Si(2)−O(2) | 1.607(2) | Si(2)−F(2) | 1.612(2) |
| Si(2)−C(15) | 1.877(4) | | |

| | | | |
|---|---|---|---|
| O(2)−Sn(1)−O(1) | 99.97(11) | O(2)−Sn(1)−C(1) | 110.14(13) |
| O(1)−Sn(1)−C(1) | 109.68(13) | O(2)−Sn(1)−C(5) | 104.72(14) |
| O(1)−Sn(1)−C(5) | 105.46(13) | C(1)−Sn(1)−C(5) | 124.1(2) |
| O(1)−Si(1)−F(1) | 107.78(14) | O(1)−Si(1)−C(11) | 111.3(2) |
| F(1)−Si(1)−C(11) | 105.0(2) | O(1)−Si(1)−Si(2a) | 110.92(10) |
| F(1)−Si(1)−Si(2a) | 106.90(10) | C(11)−Si(1)−Si(2a) | 114.45(13) |
| O(2)−Si(2)−F(2) | 108.33(14) | O(2)−Si(2)−C(15) | 111.2(2) |
| F(2)−Si(2)−C(15) | 104.6(2) | O(2)−Si(2)−Si(1a) | 110.57(10) |
| F(2)−Si(2)−Si(1a) | 106.05(10) | C(15)−Si(2)−Si(1a) | 115.57(13) |
| Si(1)−O(1)−Sn(1) | 145.0(2) | Si(2)−O(2)−Sn(1) | 147.1(2) |

| | |
|---|---|
| F(1)−Si(1)−O(1)−Sn(1) | 18.0(3) |
| O(2)−Sn(1)−O(1)−Si(1) | −147.1(3) |
| Si(1a)−Si(2)−O(2)−Sn(1) | −96.7(3) |
| Si(2a)−Si(1)−C(11)−C(14) | 179.3(3) |
| Si(2a)−Si(1)−C(11)−C(12) | −59.8(3) |
| Si(2a)−Si(1)−O(1)−Sn(1) | 98.7(3) |
| F(2)−Si(2)−O(2)−Sn(1) | 19.1(3) |
| O(1)−Sn(1)−O(2)−Si(2) | 145.8(3) |
| Si(2a)−Si(1)−C(11)−C(13) | 60.3(3) |
| Si(1a)−Si(2)−C(15)−C(18) | −68.8(3) |

$^a$ Symmetry transformation used to generate equivalent atoms: $a = -x, -y, -z$.

The H atoms were placed in geometrically calculated positions and refined with common isotropic temperature factors for the alkyl goups ($H_{alkyl}$: C−H 0.96 Å, $U_{iso}$ 0.144(14) Å$^2$ (**6**), $U_{iso}$ 0.096(3) Å$^2$ (**7**)). Disordered Cl atoms were found for the solvent molecule $CHCl_3$ in **6** at Cl(3) and C(3′) (sof 0.5).

Atomic scattering factors for neutral atoms and real and imaginary dispersion terms were taken from ref 10. The figures were created by SHELXTL-Plus.[11] Crystallographic data are given in Table 1, and selected bond distances and angles are given in Tables 2 and 3.

## Results and Discussion

**Synthetic Aspects.** The reaction of di-*tert*-butyltin oxide, **1**, with 1,2-di-*tert*-butyl-1,1,2,2-tetrachlorodisilane, **2**, afforded almost quantitatively 3,4-bis(di-*tert*-butylchlorostannoxy)-1,1,3,4-tetra-*tert*-butyl-2,5-dioxa-3,4-disila-1-stannacyclopentane, **4**, as an amorphous solid (eq 1). Compound **4** is extremely sensitive

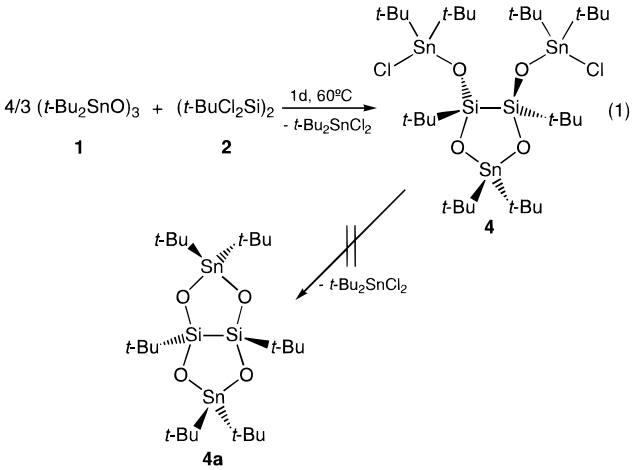


against moisture. It reacts with water to give $t$-$Bu_2Sn(OH)Cl$[12] and $t$-$Bu_2Sn(OH)_2$.[4] In solution, the latter undergoes immediate self-condensation under formation of **1**. Attempts to synthesize bicyclic **4a** from **4** by elimination of a second $t$-$Bu_2SnCl_2$ were not successful presumably because of ring strain in **4a** (eq 1).

The structure of the 2,5-dioxa-3,4-disila-1-stannacyclopentane derivative, **4**, follows unambiguously from NMR studies. Its $^{119}$Sn NMR spectrum showed two resonances with an integral ratio of 2:1 at −49.9 ($^1J(^{119}Sn-^{13}C) = 453$ Hz, $^2J(^{119}Sn-^{29}Si) = 112$ Hz) and −88.8 ppm ($^1J(^{119}Sn-^{13}C) = 467$ Hz). This chemical shift favors indeed a five-membered rather than a ten-membered ring.[2n] The $^{29}$Si NMR spectrum displayed a single resonance at −14.3 ppm with $^2J(^{29}Si-^{119}Sn)$ couplings of 112 and 12 Hz and a $^1J(^{29}Si-^{13}C)$ coupling of 65 Hz. The $^{13}$C NMR spectrum showed two Sn$C$ and two $CCH_3$ resonances at 42.4 ($^1J(^{13}C-^{119}Sn) = 456$ Hz), 41.9 ($^1J(^{13}C-^{119}Sn) = 450$ Hz), 29.9, and 29.8 ppm assigned to the carbons of the $t$-$Bu_2SnOCl$ moieties, resonances at 39.4 ($^1J(^{13}C-^{119}Sn) = 466$ Hz) and 30.2

**Table 3.** Selected Bond Lengths (Å) and Angles (deg) for **6**$^a$

| | | | |
|---|---|---|---|
| Sn(1)−O(1a) | 2.056(7) | Sn(2)−F(2) | 1.981(7) |
| Sn(1)−O(1) | 2.118(7) | Sn(2)−O(1a) | 2.077(8) |
| Sn(1)−F(1) | 2.177(6) | Sn(2)−C(15) | 2.158(13) |
| Sn(1)−C(5) | 2.199(12) | Sn(2)−C(11) | 2.193(13) |
| Sn(1)−C(1) | 2.212(12) | Sn(2)−F(1) | 2.196(7) |
| Sn(1)−F(2a) | 3.656(7) | | |

| | | | |
|---|---|---|---|
| O(1a)−Sn(1)−O(1) | 73.2(3) | C(1)−Sn(1)−F(2a) | 78.1(4) |
| O(1a)−Sn(1)−F(1) | 72.3(3) | F(2)−Sn(2)−O(1a) | 86.7(3) |
| O(1)−Sn(1)−F(1) | 145.4(3) | F(2)−Sn(2)−C(15) | 94.8(5) |
| O(1a)−Sn(1)−C(5) | 116.6(4) | O(1a)−Sn(2)−C(15) | 121.8(4) |
| O(1)−Sn(1)−C(5) | 104.8(4) | O(1a)−Sn(2)−C(11) | 118.4(4) |
| F(1)−Sn(1)−C(5) | 91.7(4) | C(15)−Sn(2)−C(11) | 118.8(5) |
| O(1a)−Sn(1)−C(1) | 124.4(4) | F(2)−Sn(2)−F(1) | 158.0(3) |
| O(1)−Sn(1)−C(1) | 105.8(4) | O(1a)−Sn(2)−F(1) | 71.5(3) |
| F(1)−Sn(1)−C(1) | 92.8(4) | C(15)−Sn(2)−F(1) | 94.3(4) |
| C(5)−Sn(1)−C(1) | 117.0(5) | C(11)−Sn(2)−F(1) | 94.2(4) |
| O(1a)−Sn(1)−F(2a) | 122.5(2) | Sn(1)−F(1)−Sn(2) | 103.6(3) |
| O(1)−Sn(1)−F(2a) | 49.4(2) | Sn(1a)−O(1)−Sn(2a) | 112.6(3) |
| F(1)−Sn(1)−F(2a) | 165.2(2) | Sn(1a)−O(1)−Sn(1) | 106.8(3) |
| C(5)−Sn(1)−F(2a) | 82.3(4) | Sn(2a)−O(1)−Sn(1) | 140.5(4) |

$^a$ Symmetry transformation used to generate equivalent atoms: $a = 1 - x, -y, -z$.

(8) Sheldrick, G. M. SHELX86. *Acta Crystallogr*. **1990**, *A46*, 467.
(9) Sheldrick, G. M. SHELXL93. University of Göttingen, 1993.
(10) *International Tables for Crystallography*; Kluwer Academic Publishers: Dordrecht, The Netherlands, 1992; Vol. C.
(11) Sheldrick, G. M. *SHELXTL-PLUS*, Release 4.1; Siemens Analytical X-ray Instruments Inc.: Madison, WI, 1991.
(12) Puff, H.; Hevendehl, H.; Höfer, K.; Reuter, H.; Schuh, W. *J. Organomet. Chem.* **1985**, *287*, 163.

ppm assigned to the carbons of the $t$-$Bu_2SnO_2$ moiety, and signals at 21.6 ($^1J(^{13}C-^{29}Si) = 64$ Hz, $^3J(^{13}C-^{119/117}Sn) = 13$ Hz) and 27.1 ppm belonging to the silicon-bonded *tert*-butyl groups. The $^1H$ NMR spectrum displayed four singlets of equal integral ratio at 1.43 ($^3J(^1H-^{119}Sn) = 109$ Hz), 1.41 ($^3J(^1H-^{119}Sn) = 107$ Hz), 1.38 ($^3J(^1H-^{119}Sn) = 97$ Hz), and 1.10 ppm ($^3J(^1H-^{29}Si) = 6$ Hz) which are assigned to the protons of the $t$-$Bu_2SnOCl$, $t$-$Bu_2SnO_2$, and $t$-$Bu_2Si_2$ moieties, respectively. Especially the number of the $^{13}C$ and $^1H$ resonances, respectively, and the integral ratios of the latter identify **4** to be the racemate form. For the meso form, five $^1H$ and ten $^{13}C$ NMR resonances would be expected. The exact connectivities of all *tert*-butyl groups have been established by gradient-enhanced 2D $^1H-^{119}Sn$ HMQC, $^1H-^{13}C$ HMQC, and $^1H-^{13}C$ HMBC experiments.[7a−c] There was no indication for formation of the corresponding meso form of **4**.

Reaction in chloroform of di-*tert*-butyltin oxide, **1**, with 1,2-di-*tert*-butyl-1,1,2,2-tetrafluorodisilane, **3**, provided almost quantitatively 5,6-difluoro-1,1,3,3,5,6-hexa-*tert*-butyl-2,4,7-trioxa-5,6-disila-1,3-distannacycloheptane, **5**, and 1,3-difluorotetra-*tert*-butyldistannoxane, **6** (eq 2). Compound **6** precipitated almost

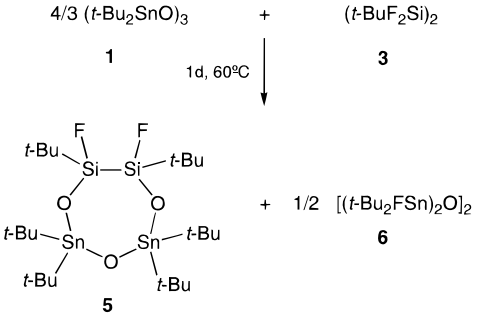


completely from the reaction mixture and was filtered off. A detailed analysis of its solution and solid-state structure is given below.

The solvent of the filtrate was evaporated to give amorphous **5** as a mixture of diastereomers which could not be separated.

The 1D {$^1H$}-decoupled $^{119}Sn$ NMR spectrum of the crude and nonfiltered reaction mixture of the reaction according to eq 2 showed two resonances at −121.2 ppm ($^2J(^{119}Sn-^{117}Sn) = 612$ Hz, $^2J(^{119}Sn-^{29}Si) = 75$ Hz, $^1J(^{119}Sn-^{13}C) = 513$, 497 Hz) and −126.8 ppm ($^2J(^{119}Sn-^{117}Sn) = 712$ Hz, $^2J(^{119}Sn-^{29}Si) = 76$ Hz), respectively, with an integral ratio of 1:0.03.

We tentatively assign the major resonance to the racemate form of **5** and the minor resonance to the meso form of **5**. Also present were a broad resonance at −95.4 ppm ($W_{1/2}$ 200 Hz) (integral 0.18) which is assigned to 1,1,3,4,6,6,8,9-octa-*tert*-butyl-3,4,8,9-tetrafluoro-2,5,7,10-tetraoxa-3,4,8,9-tetrasila-1,6-distannacyclodecane, **7** (see below), two triplets at −226.3 (integral 0.03) and −290.4 ppm (integral 0.03), respectively, which are assigned to 1,3 difluorotetra-*tert*-butyldistannoxane **6** (see below), and further minor resonances at −52.0, −149.6, −154.3, −157.7, −161.5, and −166.2 ppm (total integral 0.1) for which no assignment was made.

The $^{29}Si$ NMR spectrum of the same solution displayed two doublets of doublets centered at −7.3 ppm ($^1J(^{29}Si-^{19}F) = 354$ Hz, $^2J(^{29}Si-^{19}F) = 54$ Hz) (**7**) and −12.0 ppm ($^1J(^{29}Si-^{19}F) = 346$ Hz, $^2J(^{29}Si-^{19}F) = 58$ Hz), $^2J(^{29}Si-^{117/119}Sn) = 74$ Hz) (**5**, racemate). The $^{19}F$ NMR spectrum showed two resonances at −134.2 ppm (**5**, racemate) and at −139.8 ppm (**7**).

When the reaction according to eq 2 was performed with $^5/_3$ ($t$-$Bu_2SnO)_3$, followed by filtration of **6**, evaporation of the solvent, and partial redissolving of the residue in $CDCl_3$, the

**Chart 1**

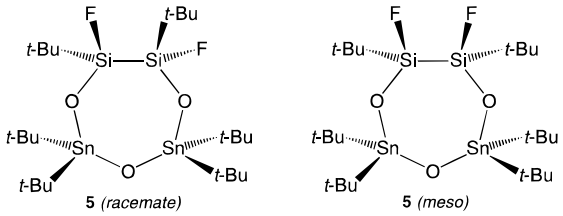


**Chart 2**

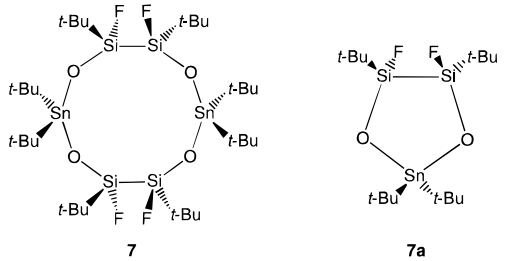


$^{119}Sn$ NMR spectrum showed only the resonances for **5** (racemate and meso with an integral ratio of 2:1) (see Chart 1) and a resonance at −84.0 ppm ($^2J(^{119}Sn-O-^{117}Sn) = 370$ Hz, integral 0.5) assigned to di-*tert*-butyltin oxide, **1**. In fact, the meso form was enriched by a lucky coincidence which allowed its unambiguous identification.

The $^{29}Si$ NMR spectrum of this solution displayed two doublets of doublets centered at −13.0 ppm ($^1J(^{29}Si-^{19}F) = 346$ Hz, $^2J(^{29}Si-^{19}F) = 43$ Hz) (**5**, meso) and −12.1 ppm ($^1J(^{29}Si-^{19}F) = 345$ Hz, $^2J(^{29}Si-^{19}F) = 58$ Hz, $^2J(^{29}Si-^{117/119}Sn) = 74$ Hz) (**5**, racemate). The $^{19}F$ NMR spectrum showed two resonances at −136.4 ppm (**5**, racemate) and at −138.0 ppm (**5**, meso), respectively, with an integral ratio of 2:1.

The $^{13}C$ NMR spectrum showed two Sn*C* and two C*C*$H_3$ resonances at 38.83, 38.77, 30.10, and 29.60 ppm assigned to **5** (racemate) and two Sn*C* and two C*C*$H_3$ resonances at 39.70, 38.60, 30.03, and 29.98 ppm assigned to **5** (meso). The signals for the silicon-bonded *tert*-butyl groups appear at 20.7 (Si*C*), 25.4 (SiC*C*$H_3$, meso), and 25.2 (SiC*C*$H_3$, racemate) ppm. Also present were signals at 38.1 and 30.6 ppm assigned to **1**.

In addition to $^2J(^{119}Sn-O-^{117}Sn)$ couplings, the Sn−O−Sn bridge in **5** was further confirmed from long-range $^5J(^1H-^{119}Sn)$ correlations (∼2 Hz) observed between both $t$-$Bu_2Sn$ moieties in the ge-$^1H\{^{119}Sn\}$ HMQC spectrum.

When a hexane solution containing the 2,4,7-trioxa-5,6-disila-1,3-distannacycloheptane derivative, **5**, and residual traces of the distannoxane **6** was filtered through filter aid, formation of 1,1,3,4,6,6,8,9-octa-*tert*-butyl-3,4,8,9-tetrafluoro-2,5,7,10-tetraoxa-3,4,8,9-tetrasila-1,6-distannacyclodecane, **7**, was observed. Its molecular structure is shown in Chart 2.

Formation of **7** can be rationalized formally by extrusion of a [$t$-$Bu_2SnO$] unit from the 2,4,7-trioxa-5,6-disila-1,3-distannacycloheptane derivative, **5**, followed by dimerization of the resulting five-membered ring **7a**. In solution, **7** forms the five-membered ring **7a**. This is supported by osmometric molecular weight determination in $CHCl_3$ and the $^{119}Sn$ chemical shift of −95.0 ppm, which is comparable to those of six-membered [($t$-$Bu_2SnO$)($Ph_2SiO$)$_2$] ($\delta(^{119}Sn)$ −119.5 ppm)[2n] and five-membered **4** (see above) but quite different from those of eight-membered [($t$-$Bu_2SnO$)($t$-BuFSiO)]$_2$ ($\delta(^{119}Sn)$ −161.5/−163.1 ppm).[4]

**Molecular Structure of 7.** The molecular structure of **7** is shown in Figure 1. A view along the Si−Si axis is depicted in

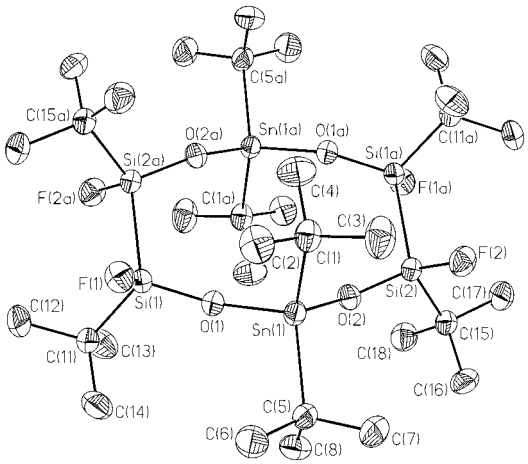


**Figure 1.** General view (SHELXTL-PLUS) of a molecule showing 30% probability displacement ellipsoids and the atom-numbering scheme for **7**. (Symmetry transformations used to generate equivalent atoms: $a = -x, -y, -z$.)

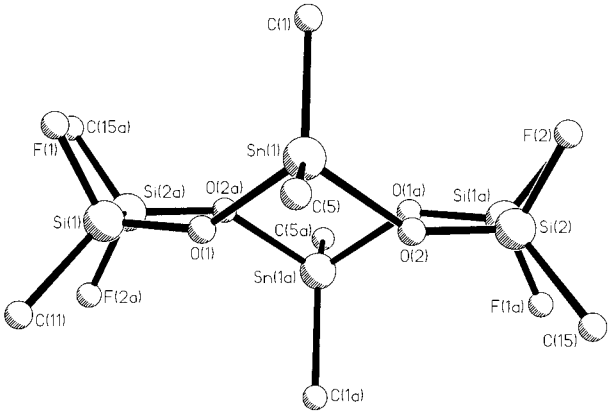


**Figure 2.** General view (SHELXTL-PLUS) through the planar plane for **7**. (Symmetry transformations used to generate equivalent atoms: $a = -x, -y, -z$.)

Figure 2. Selected bond lengths, bond angles, and torsion angles are given in Table 2.

Compound **7** is a centrosymmetric 10-membered ring composed of four Si, four O, and two Sn atoms. The four O and four Si atoms form an almost perfect plane (mean deviation 0.018 Å) from which the Sn(1)/Sn(1a) atoms are elongated above and below by 1.043 Å. The exocyclic fluorine atoms are all trans. The conformation along the Si−Si bond is almost perfectly eclipsed (F(1)−Si(1)−Si(2a)−C(15a) −13.7(2)°). The silicon as well as the tin atoms show distorted tetrahedral configurations with the distortions caused by the bulky *tert*-butyl groups. All bond lengths are as expected and comparable with those of related compounds.[2]

**Molecular Structure of 6.** The molecular structure of **6** is shown in Figure 3. Selected bond lengths and bond angles are listed in Table 3.

The molecule exhibits a centrosymmetric dimer with a typical ladder-type arrangement comparable with that of $[(R_2ClSn)_2O]_2$ (R = Me, *i*-Pr, Ph).[13] The $Sn_4O_2F_4$ atoms are planar to ±0.044 Å. Each tin atom exhibits a distorted trigonal bipyramidal

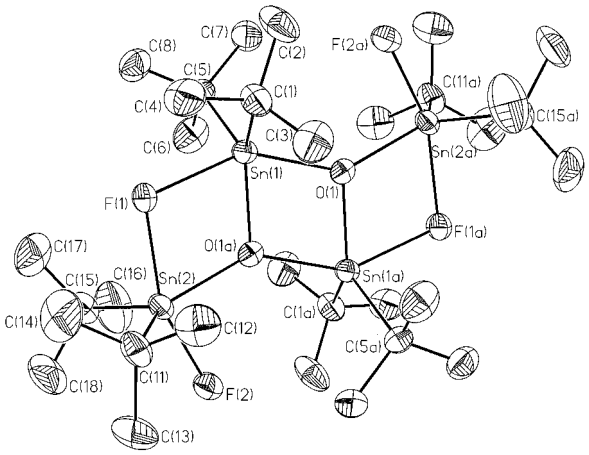


**Figure 3.** General view (SHELXTL-PLUS) of a molecule showing 30% probability displacement ellipsoids and the atom-numbering for **6**. (Symmetry transformations used to generate equivalent atoms: $a = 1 - x, -y, -z$.)

geometry (geometrical goodness[14] $\Delta\Sigma(\varphi)$ 74.2 (Sn(1)), 78.7° (Sn(2)); ΔSn(plane) 0.173(7) Å (Sn(1)), 0.128(7) Å (Sn(2))). Both Sn(1) and Sn(2) are each coordinated by two *t*-Bu groups and by O(1a) in equatorial positions. The axial positions at Sn(1) and Sn(2) are occupied by O(1) and F(1) and by F(1) and F(2), respectively. The Sn(1)−F(1)−Sn(2) bridge is nearly symmetric with Sn−F distances comparable to those found for $[(Ph_2ClSnCH_2)_2F]^-[Et_4N]^+$.[15] The terminal Sn(2)−F(2) distance is almost identical to an Sn−F single bond length (1.96 Å)[16] whereas the Sn(1)−F(2a) distance of 3.656(8) Å is too large to be considered as an interaction. In the lattice, there are no intermolecular contacts.

**Solution NMR of 6.** Once isolated, **6** is almost insoluble in common organic solvents such as chloroform, dichloromethane, or toluene. Thus, a reasonable $^{119}$Sn NMR spectrum could be obtained only from the crude reaction mixture in which it appears to be more soluble (eq 2). In addition to the signals assigned to **5** (see discussion above), the $^{119}$Sn NMR spectrum displayed two triplets of low intensity with an integral ratio close to 1 at −226 ppm ($W_{1/2}$ 30 Hz) ($^1J(^{119}Sn-^{19}F) = 807$, $^2J(^{119}Sn-O-^{119/117}Sn) = 110$ Hz) and at −290 ppm ($W_{1/2}$ 18 Hz) ($^1J(^{119}Sn-^{19}F) = 2450$, $^2J(^{119}Sn-O-^{119/117}Sn) = 110$ Hz), respectively.

The $^{19}$F NMR spectrum of the reaction mixture showed numerous overlapping minor resonances, making an unambiguous assignment very difficult. However, a $^{19}F-^{117}Sn$ HMQC experiment[7]—performed with the $^{117}$Sn nucleus rather than the $^{119}$Sn nucleus for reasons of local radio interferences—revealed that the two above-mentioned tin resonances are correlated with a single $^{19}$F resonance at −139.8 ppm. The $^{19}F-^{117}Sn$ HMQC correlation peak at low $^{117}$Sn frequency exhibited one pair of $^1J(^{19}F-^{117}Sn)$ splittings (2340 Hz), and the one at high $^{117}$Sn frequency two such pairs (840 and 704 Hz). The 1D$^{19}$F {$^1$H} NMR spectrum (Figure 4) of crystalline **6** displayed a single resonance at −139.8 ppm with well-resolved $^1J(^{19}F-^{119/117}Sn)$ satellites of (I) 2442/2335, (II) 874/834 and (III) 743/709 Hz, respectively, and unresolved $^nJ(^{19}F-^{119/117}Sn)$ satellites of (IV) 65 Hz.

The I satellite splittings are in agreement with the $^1J(^{119}Sn-^{19}F)$ value of 2450 Hz found from the $^{119}$Sn spectrum of the

(13) (a) Dakternieks, D.; Gable, R.; Hoskins, B. F. *Inorg. Chim. Acta* **1984**, *85*, L43. (b) Harrison, P. G.; Begley, M. J.; Molloy, K. C. *J. Organomet. Chem.* **1980**, *186*, 213. (c) Puff, H.; Friedrichs, E.; Visel, F. *Z. Anorg. Allg. Chem.* **1981**, *477*, 50. (d) Vollano, J. F.; Day, R. O.; Holmes, R. R. *Organometallics* **1984**, *3*, 745.

(14) (a) Dräger, M. *J. Organomet. Chem.* **1983**, *251*, 209. (b) Kolb, U.; Beuter, M.; Dräger, M. *Inorg. Chem.* **1994**, *33*, 4522.

(15) Dakternieks, D.; Jurkschat, K.; Zhu, H.; Tiekink, E. R. T. *Organometallics* **1995**, *14*, 2512.

(16) Kolb, U.; Dräger, M.; Jousseaume, B. *Organometallics* **1991**, *10*, 2737.

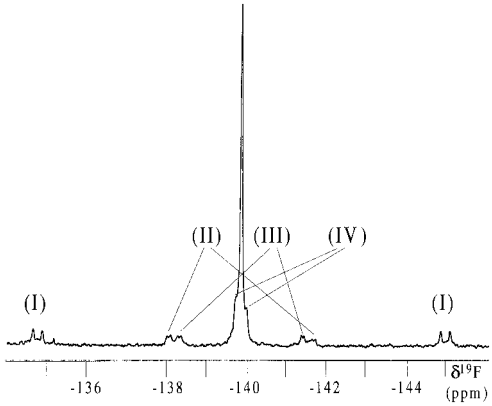


**Figure 4.** Proton-decoupled $^{19}$F NMR spectrum of **6** in $CD_2Cl_2$ at room temperature. I−IV refer to the $^1J(^{117/119}Sn-^{19}F)$ and $^3J(^{117/119}Sn-^{19}F)$ couplings, respectively (see text).

mixture. By contrast, the II and III satellite splittings do not match the single $^1J(^{119}Sn-^{19}F)$ value of 807 Hz from the $^{119}$Sn spectrum of the mixture, but the average of the $^1J(^{19}F-^{119}Sn)$ coupling splittings of the II and III satellites, 809 Hz, is equal to this value within experimental error. Moreover, the sum of the intensities of the satellites II and III is equivalent to the intensity of the I satellites, as assessed by line-shape simulation (PERCH).[7c]

These findings are rationalized as the I satellites being exchange averaged and the II and III ones being not. The presence of a $^{119}$Sn triplet in the $^{119}$Sn spectrum of the mixture rather than a doublet of doublets with II and III $^1J(^{119}Sn-^{19}F)$ splittings is ascribed to a slightly faster time scale in the $^{119}$Sn NMR spectrum of the crude reaction mixture than in the $^{19}$F NMR spectrum of pure **6**. Different exchange rates in reaction mixture and pure compound are not unrealistic, given, for instance, the better solubility of **6** in the former than in the latter.

A nonrigid structure **B**/**B′**, as proposed in Scheme 1, explains both the observed $^1J(^{19}F-^{119/117}Sn)$ patterns and the exchange averaging. The rigid structure **A** observed in the crystalline state is shown for comparison.

In a fully rigid type **B** (or **B′**) structure, four different types of $^1J(^{19}F-^{119/117}Sn)$ couplings should be expected, given the pairs of Sn(1)−F(a), Sn(1)−F(b), Sn(2)−F(a), and Sn(2)−F(b) bonds. The (I) 2442/2335 Hz satellites are assigned to the $^1J(^{19}F-^{119/117}Sn)$ couplings of the Sn(2)−F(a) and Sn(2)−F(b) bond pairs which are time scale averaged. The two smaller nonaveraged (II) 874/834 and (III) 743/709 Hz satellites are assigned to the pairs Sn(1)−F(a) and Sn(1)−F(b), respectively. These data, as well as the simultaneous presence of a single $^{19}$F resonance and two $^{119}$Sn triplets, can be explained by the equilibrium between the valence tautomers **B** and **B′** interconverting through the time scale averaged structure (**C**) as a transition state (or less likely an intermediate) (Scheme 1). The differentiated averaging behavior can be rationalized as follows: (i) The difference of the $^{19}$F chemical shifts of F(a) and F(b) in **B**/**B′** is small with respect to the rate constant of the valence tautomerization process (averaged $^{19}$F chemical shift). (ii) The same holds for the difference between the $^1J(^{19}F-^{119/117}Sn)$ couplings of the Sn(2)−F(a) and Sn(2)−F(b) bonds averaging to the I satellites, which is ascribed to sufficiently similar bond lengths (X-ray: 2.196(7) and 1.981 (7 Å) and chemical environments to achieve this averaging on the $^{19}$F time scale. A rigid structure with accidentally identical $^1J(^{19}F-^{119/117}Sn)$ couplings is also an explanation but appears less likely. (iii) By contrast, the difference between the $^1J(^{19}F-^{119/117}Sn)$ couplings of the Sn(1)−F(a) and Sn(1)−F(b) bonds is now

**Scheme 1.** Valence Tautomerization Process in **6**[a]

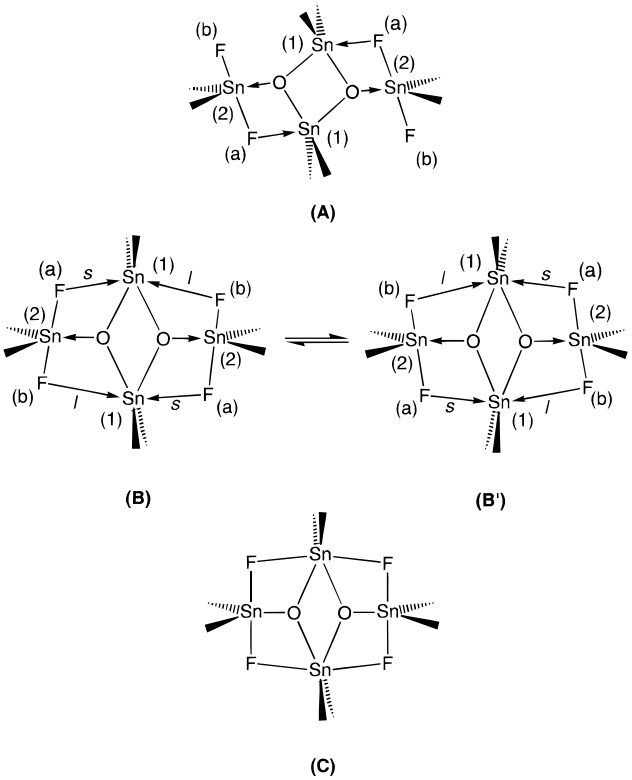


[a] The *tert*-butyl groups are omitted for clarity. The labels *l* and *s* refer to "long" and "short", respectively.

sufficiently large for the averaging of the II and III satellites to be not achieved on the $^{19}$F NMR time scale, being due to sufficiently different Sn(1)−F(a) and Sn(1)−F(b) contacts (X-ray: 2.177(6) and 3.656 (7 Å).

In this interpretation, the X-ray structure **A**, as viewed in Chart 3, is a limiting case of **B′** where the Sn(1)−F(b) bond is nonexistent. Actually, the very low $^1J(^{19}F-^{119/117}Sn)$ couplings for II and III satellites as compared to the I satellites suggest that, in solution, both Sn(1)−F(a) and Sn(1)−F(b) contacts of **B**/**B′** are very weak, the coupling constants of similar order of magnitude pointing toward a smaller bond length difference between Sn(1)−F(a) and Sn(1)−F(b) in solution than in the crystalline state.

The correctness of this interpretation is confirmed by the observation that, in toluene-$d_8$ at 328 K, the $^1J(^{19}F-^{117/119}Sn)$ satellite coupling splittings II and III finally also enter into precoalescence, only two broad $^{117/119}$Sn unresolved satellite pairs being now observed with apparent coupling splittings of 833 and 737 Hz, instead of averaged 854/726 Hz at room temperature. Above 333 K, the $^{19}$F NMR spectrum becomes immeasurable because of decomposition.

In fact, the valence tautomer interconversion of **B** and **B′** in **6** represents a unique example where, for the first time, the "motion of electron density" in a hypervalent system becomes visible by NMR spectroscopy, because it is accompanied by a back and forth motion (a kind of wagging) of fluorines a and b which are exchanging their environments (Scheme 1). Thus, the averaged structure **C** is in complete agreement with all time scale averaged $^{119}$Sn and $^{19}$F NMR spectral data.

Interestingly, the chloro-substituted analogue of **6**, i.e., $[t\text{-}Bu_2\text{-}ClSnOSnCl\text{-}t\text{-}Bu_2]_2$, does not exist.[17] We attribute this difference to the higher bridging capacity of fluoride in comparison with chloride.

Compound **6** is extremely sensitive to moisture and reacts quantitatively with air moisture under formation of [*t*-$Bu_2Sn(OH)F]_2$,[12] referred to as **6a**. The identity of the latter was confirmed by elemental analysis and an IR spectrum ($\nu$OH 3084 $cm^{-1}$) being identical with those of an authentic sample of **6a**.[12]

**Acknowledgment.** We thank the Deutsche Forschungsgemeinschaft, the Fonds der Chemischen Industrie, and the Martin Schmeisser Stiftung of Dortmund University for financial support. We also acknowledge R. Kinne and B. Griewel from the Max Planck Institute for Molecular Physiology Dortmund for recording selected 29Si and 119Sn NMR spectra (J.B., M.S., K.J.). The financial support of the Belgian National Science Foundation (FKFO, Grant 2.0094.94), of the Belgian Nationale Loterij (Grant 9.0006.93), and of the Fund for Scientific Research—Flanders (Belgium) (FWO, Grant G.0192.98) is gratefully acknowledged (R.W., M.B.). J.C.M. is a Postdoctoral Researcher of the Fund for Scientific Research—Flanders (Belgium). In addition, partial financial support by the European Human and Capital Mobility Program (Contract ERBCHRX-CT94-0610) is acknowledged (K.J., R.W.).

**Supporting Information Available:** Tables of atomic coordinates, anisotropic displacement parameters, bond lengths and angles, torsion angles, least-squares plane data, and complete crystallographic data for **6** and **7** (15 pages). Ordering information is given on current masthead page.

IC971504+

(17) Dakternieks, D.; Jurkschat, K.; van Dreumel, S.; Tiekink, E. R. T. *Inorg. Chem* **1997**, *36*, 2023.